Geochemical trends in evaporative tailings ponds – an experimental study

Timo Kirchner[1], Nicole Marsh[1], Bruce Mattson[1]

[1]*Lorax Environmental Services Ltd., 2289 Burrard St., Vancouver, BC, V6J 3H9, Canada*

Abstract

Environmental best practices and practical considerations commonly require mines to store process water in large reservoirs such as tailings ponds. In many jurisdictions, mining companies need to demonstrate an understanding of the geochemical evolution and environmental impact of such reservoirs. The development of predictive mine drainage chemistry models is commonly complicated by the highly variable geochemical behaviour of the different dissolved constituents in contact with exposed mine materials. In dry environments, the geochemistry of tailings ponds may be driven by evapo-concentration where certain dissolved species become more strongly enriched than others. This discrepancy is especially evident in neutral environments where the concentrations of many species are solubility-controlled.

To better understand the relative attenuation mechanisms occurring in an evaporative tailings pond, a small-scale (30L) laboratory pond was subjected to approximately 96% evaporation where seven water samples were collected and analyzed at different evaporation steps over a time period of 21 days. The experimental pond water was in contact with a layer of non-acid generating tailings to provide nucleation and adsorption sites. Measured and theoretical concentration factors for several species were calculated and compared at each evaporation step to put the brine evolution into context.

The pH remained circum-neutral and increased slightly from 7.7 to 8.2 over the course of the experiment. Decreasing redox conditions were indicated by an increasing NO_2/NO_3 ratio. Other geochemical trends with degree of evaporation suggested that Ca and alkalinity were limited by calcite precipitation early on, while Ca and sulphate precipitated as gypsum during slightly more evolved stages of the test. Visible gypsum did in fact form on the pond surface, consistent with the timing of the geochemical signature. Other major cations (K, Na, Mg) behaved conservatively. The geochemical behaviour of dissolved trace metals and metalloids was variable. Base metals Cu, Co, N, and Zn were effectively scavenged by co-precipitation and/or adsorption onto secondary phases, most likely Fe-hydroxides. Metalloids that form oxy-anionic complexes were attenuated (As, Sb) or behaved conservatively (Mo, Se) becoming progressively enriched in the evolving brine. For Mo in particular, the dissolved geochemical load increased as the pond water became more brine-like. This is interpreted to be a result of desorption or other mobilizing processes releasing Mo from the material in response to the slight increase in pH. Comparison of the apparent mass loadings removed from solution with the elemental budget in the secondary precipitate indicates that, especially for strongly solubility-controlled species, ion exchange between tailings and water occurs to attain or approach geochemical equilibrium. These results give new insight into the relative solubilities of various species in neutral evaporative tailings ponds, highlighting the effect of minor changes in the ambient regime (e.g., pH, Eh) on the aqueous geochemical composition.

Evapo-concentration, tailings pond, mine drainage, aqueous geochemistry, adsorption

Introduction

Tailings storage facilities (TSFs) are integral components of many mining operations and can cover many square kilometers of land, causing these facilities to have a major impact on the local water balance. Various types of tailings disposal strategies exist (e.g., tailings slurry deposition, dry stack, etc.) where TSF designs are commonly governed by site geographical constraints, climate, and environmental considerations. Where tailings are deposited in the form of a slurry, tailings ponds commonly form and inundate portions of the settled tailings. The surface area of such tailings ponds can vary significantly seasonally as new tailings are added and as a result of precipitation and evaporation. Environmentally,

establishing a pond in the TSF can be advantageous as it increases the proportion of wetted tailings, which inhibits the oxidation of pyrite and, therefore, acid production. However, tailings ponds may serve as a water source for mining or other (e.g., agricultural irrigation) purposes and become part of the local ecosystem long-term. Therefore, the prediction of the geochemical and hydrogeological regime is crucial, and most commonly a regulatory requirement, to avoid contaminant transport into the receiving environment. Particularly in arid climates, evaporation will strongly affect the TSF pond water reservoir leading to the enrichment of dissolved geochemical species, sometimes to brine-like concentration levels. Due to the highly variable behavior and saturation indices of the various dissolved species, modelling the geochemistry of an evolving evaporative water body in contact with fine-grained tailings solids can be challenging. Previous studies investigating the effect of evapo-concentration on water chemistry have largely focused on major elemental trends in salt lakes (e.g., Deocampo & Jones 2013), however little is known about the geochemical evolution of minor and trace elements in such systems. To gain an understanding of the mechanisms controlling the geochemistry of evaporating tailings ponds for parameters that are commonly of concern in mine drainage, a small-scale experiment simulating an evaporating tailings pond was conducted. The results of this study are intended to help constrain solubility maxima, the relative timing of reaching the latter as well as mechanisms controlling tailings-water interactions.

Methods

The tailings pond was simulated by filling an acid-cleaned, chemically resistant polyethylene (49 L) tub with 7.1 kg of a dry tailings composite and 30.2 kg of tailings supernatant (fig. 1). Once the tailings material had completely settled, a water sample was collected to determine the initial pond-water chemistry.

In the initial stages of the experiment, three 100 watt lamps were installed facing the analogue pond to accelerate evaporation. For the final experiment configuration, a 900/1500 watt fan heater was used to accelerate evaporation.

Evaporation was monitored by weighing the container and calculating the mass lost by evaporation. Eight ~100 mL samples were collected from the pond at various evaporation stages of the experiment. The timing of sample collection was based on geochemical and practical constraints, where a geochemical speciation model (PHREEQC) was run to identify residual water volumes at which evaporation would have a relevant geochemical effect that can be used for TSF considerations. Sample volumes and corresponding evaporation stages are reported in Table 1.

The water samples were extracted from the top of the experimental pond using a clean syringe and filtered using a 45 µm syringe filter. Samples were tested at the Lorax lab for pH, alkalinity, and conductivity. A sample aliquot was also preserved in-house and sent to ALS Laboratories in Burnaby, BC for analysis of anions, total-phosphate, dissolved metals and acidity.

Between the second and third sampling event grains of light-coloured, flaky precipitates were observed on the water surface. These aggregates grew in diameter over the course of the experiment and eventually sank to the bottom of the experimental container. After the last water sample was collected, the tailings were allowed to air-dry completely. Precipitate flakes (19 g) were extracted from the top of the tailings using acid-cleaned plastic tweezers (fig. 1). The precipitate was sent to SGS Laboratories in Burnaby, BC for solid-phase analysis (aqua regia digest with ICP-MS finish).

Table 1 *Sampling schedule and volumes*

Sampling Step	Date Sampled	Total Mass Before Sample (kg)	Sample Taken (L)	Evaporated
0	March-04-15	38	0.11	0%
1	March-13-15	25	0.11	44%
2	March-18-15	19	0.11	68%
3	March-20-15	15	0.11	79%
4	March-23-15	14	0.11	85%
5	March-24-15	13	0.095	89%
6	March-24-15	11	0.10	93%
7	March-25-15	10	0.12	96%

Figure 1 *Bench-scale experimental tailings pond (left) and precipitate on top of dry pond (right)*

Results and Discussion

Ongoing evaporation of a standing water body will result in the oversaturation and attenuation of most, if not all species at different points in time and at different levels. Analytical results of the water chemistry at the various evaporation steps are provided in Table 2. The geochemical composition of the tailings material in contact with the experimental pond water is given in Table 3. To put the experimental results into context for each species, measured concentrations were compared to modelled values that would be expected if no solubility limits existed. These theoretical concentrations were calculated incrementally as a function of evaporation based on the assumption that all dissolved species accumulate linearly proportional to the amount of water being lost. For this, a concentration factor needs to be defined for each calculation step to account for the amount of geochemical load being lost during the water sampling events. In a very general sense, this can be written as

$$F_{tx} = C_{sx}/C_{s0} \qquad \text{(eq. 1)}$$

where F_{tx} is the theoretical concentration factor at evaporation step x, C_{sx} is the dissolved concentration of species s at the same evaporation step, and C_{s0} is the initial dissolved concentration of species s. Since water is being removed for sampling, the cumulative concentration factor is the product of the incremental concentration factors F_{ti} that have to be calculated for each evaporation step:

$$F_{tx} = \prod F_{ti} \qquad \text{(eq. 2)}$$

The theoretical incremental concentration factor F_{ti} can be calculated as a function of the evaporative water loss between each sampling cycle which, in turn, can be derived based on the water sample volumes extracted:

$$F_{ti} = 1/[1-(V_e/(V_r-V_s))] \qquad \text{(eq. 3)}$$

where V_e, V_r, and V_s are the water volumes evaporated, remaining in experiment, and sampled, respectively. The cumulative theoretical concentration factor F_{yx} can then be compared with the measured concentration factor F_{mx} at the same evaporation step x, calculated as

$$F_{mx}= C_{mx}/C_{m0} \qquad \text{(eq. 4)}$$

where C_{m0} and C_{mx} and are the measured initial and evolved concentrations at evaporations step x, respectively. In general, it can be expected that $F_{mx} < F_{tx}$, due to secondary mineral controls and/or adsorption mechanisms in the natural system. The closer F_{mx} approaches F_{tx}, the more conservative the according dissolved species behave.

Table 2 *Geochemical composition of water samples collected at different evaporation steps during the tailings pond experiment*

Evap. step	0	1	2	3	4	5	6	7
Water volume (L)	29	16	9.2	6.0	4.2	3.2	1.8	1.1
% evaporated	0%	44%	68%	79%	85%	89%	93%	96%
pH	7.73	7.88	7.97	7.96	8.04	N/A	8.09	8.21
Alkalinity	62	103	12	10	151	#N/A	234	283
SO_4	1750	3070	3110	3290	3270	3450	4320	5970
Cl	109	193	325	469	610	744	1010	2010
NO_3	1.2	1.9	3.1	4.4	6.2	7.7	10	21
NO_2	0.022	0.29	0.62	0.95	1.0	1.2	1.5	2.8
Al	0.0037	0.0032	0.0079	<0.0025	0.0053	0.0031	0.0040	0.0053
Sb	0.0037	0.0054	0.0071	0.0093	0.0093	0.0095	0.014	0.021
As	0.0024	0.0026	0.0033	0.0043	0.0044	0.0045	0.0064	0.0087
Cd	0.000022	<0.000025	0.000033	<0.000025	<0.000025	<0.000025	0.000044	0.000035
Ca	602	1090	905	859	724	656	841	653
Co	0.0014	0.0037	0.0057	0.0070	0.0074	0.0074	0.010	0.014
Cu	0.0069	0.014	0.021	0.021	0.022	0.023	0.031	0.042
Fe	<0.002	<0.005	<0.005	<0.005	<0.005	<0.005	<0.005	0.0090
Pb	0.000042	<0.000025	0.000032	<0.000025	0.000047	<0.000025	0.000029	0.000074
Mg	48	103	165	263	355	361	590	1080
Mo	0.047	0.17	0.33	0.52	0.69	0.80	1.3	2.7
Ni	0.0041	0.0066	0.0093	0.012	0.013	0.012	0.018	0.026
K	30	59	90	129	167	171	255	393
Se	0.0026	0.0059	0.0096	0.015	0.021	0.024	0.037	0.076
Na	58	106	161	258	345	376	563	1110
Zn	<0.001	<0.0025	<0.0025	<0.0025	<0.0025	<0.0025	<0.0025	<0.0025

Notes: all concentrations are given in mg/L; alkalinity is reported in units of mg $CaCO_3$/L

A comparison of F_{mx} and F_{tx} is plotted for dissolved anions in Figure 2a with increasing values on the x-axis being equivalent to increasing water loss volumes where the circles on the curves represent evaporation steps x. The highest theoretical concentration factor has a value of 22.9, corresponding to an evaporative water loss of 96%. Sulphate becomes solubility-limited at relatively low evaporative water losses, Cl and NO_3 behave nearly conservatively. Alkalinity shows a decrease in the measured concentration factor which can be interpreted to be a result of both atmospheric equilibration and carbonate precipitation. In later stages of the experiment, this parameter closely follows the trend observed for sulphate. In this context, it should be noted, however, that pH systematically increases from 7.7 to 8.2 throughout the course of the experiment. Interestingly, measured NO_2 concentrations increase much more dramatically than predicted by the theoretical model suggesting that this anion becomes relatively enriched by other processes in addition to evapo-concentration. This is interpreted to be a result of the lower solubility of oxygen in highly saline water leading to more reducing conditions in the tailings contact water with water evaporation. The same effect would be caused by an increasing temperature which is to be expected in an evaporating water pool exposed to heat lamps. In natural systems, the decrease of redox potential may also be related to the metabolism of organic matter by heterotrophic bacteria which in turn drive oxygen consumption (Deocampo & Jones 2013). It should be noted that the loss of NO_3 strongly outweighs the increase of NO_2 concentrations, such that an overall loss of nitrogen load is observed, likely through denitrification or adsorption.

Previous studies have found that compositional trends in evaporative environments can be traced based on major anionic concentrations (e.g., Hutchinson 1957), where evolving brines tend to lose alkalinity and sulphate over time, as chloride is enriched. This trend is consistent with observations from the laboratory experiment, in which chloride behaves the most conservatively among these three anions (fig. 2a).

Major cation concentrations are generally controlled by the contact material (i.e., tailings) and mineral saturation indices in the evaporating waters. Due to its high solubility, Na is by far the most common cation in evolving brines of evaporative, natural salt lakes. Magnesium, Na, and K, all follow relatively similar concentration trajectories, where Mg falls closest to the 1:1 line (fig. 2b), suggesting that this species is evapo-concentrated conservatively with little or no mass loss to mineral precipitates or adsorption. Evidently, the major cation removal mechanism is that of calcite and gypsum precipitation as Ca increases only slightly in the first sampling cycle after which it is being removed from solution as solubility limits are reached. This is consistent with both sulphate and alkalinity following similar trends (fig. 2b). The dip in the alkalinity curve relatively early on in the experiment can therefore be explained by the rapid crystallization of calcite, directly followed by gypsum/anhydrite saturation and re-equilibration of alkalinity with the atmosphere. This is consistent with the theoretical mineral precipitation sequence observed in most saline lake regimes (e.g., Deocampo & Jones 2013) and the first visible occurrence of flaky mineral precipitates at the water surface between evaporation steps 2 and 3 (fig. 1). Commonly, in natural brines Mg-rich calcite and dolomite is precipitated before gypsum saturation is attained, however, this depends on the Mg/Ca ratio as well as the availability of CO_3 in solution. The supernatant water used for the experiment has a relatively high initial concentration of both Ca and SO_4, likely causing an earlier onset of gypsum precipitation than would be expected in natural waters and therefore suppressing Mg saturation. The concurrent 'kink' in Mg, Na, and K concentration factors between evaporation steps 4 and 5 may be an analytical artifact or the co-precipitation of these species in a pulse of a Ca-phase crystallization, but the trajectory of the trend line suggests it is unlikely to be caused by the precipitation of discrete Mg-, Na-, K-bearing minerals.

It is known that many dissolved trace metals that may be of environmental concern in neutral mine drainage are strongly attenuated through adsorption and co-precipitation while others remain in solution over a relatively wide range of pH and redox conditions (Chapman et al. 1983; Cravotta & Trahan 1999). Hydrous ferric oxides (HFO) and Al-hydroxides are highly insoluble under oxidizing, circum-neutral conditions and, especially the former, have been shown to represent a major sink for dissolved trace metals, mostly due to their amorphous nature and large surface area. Both Al and Fe are actively being removed from solution as indicated by the consistently low concentrations below detection limit (Fe) or within a factor of two of their initial concentration (Al) in the most concentrated solution. Only after the last evaporation step does Fe have a detectable concentration of 0.009 mg/L, possibly a result of the increasingly reducing conditions and the higher relative proportion of the more soluble Fe^{2+} versus Fe^{3+}. A F_{mx}-over-F_{tx} plot for Co, Cu, and Ni is shown in Figure 2c, and illustrates that attenuation mechanisms are efficiently scavenging these metals after evaporation step 3 (79% water loss) leading to a flattening of the curves. A slight increase in concentration is nevertheless observable as water continues to be evaporated.

Metalloids such as As, Mo, Se, and Sb are commonly the most problematic parameters in neutral mine drainage as they form anionic complexes in solution which are not easily adsorbed at low H^+-activities. A bimodal trend is evident for measured concentration factors of these species in Figure 2d, where As and Sb become attenuated, while Se and Mo are slightly to moderately enriched in the evaporating solution. The latter process is only possible if a geochemical load from the tailings material is in fact added to the aqueous phase. This indicates that, in response to changing geochemical conditions in the evolving brine, Mo and to a lesser degree Se loads, are not only kept in solution but have increased solubility as the tailings contact water undergoes evapo-concentration. The most plausible explanation for this trend is the slight increase in pH over the course of the experiment leading to a suppression of selenate and molybdate adsorption capacities and therefore, leading to the solubilization of these species from the tailings material. The sensitivity of Se and Mo solubility to pH in a circum-neutral regime is well-documented by several adsorption studies (e.g., Balistrieri & Chao 1990).

As the evaporating tailings contact water evolves into a progressively more saline brine, it becomes supersaturated with respect to certain species. As shown in Figure 1, a flaky, colourless precipitate formed at the water surface between evaporation steps 2 and 3. These crystals grew in diameter over the course of the experiment and eventually sank to the tailings-water interface. After termination of the experiment, this phase was sampled and submitted for solid-phase (aqua regia digest) analysis. One way

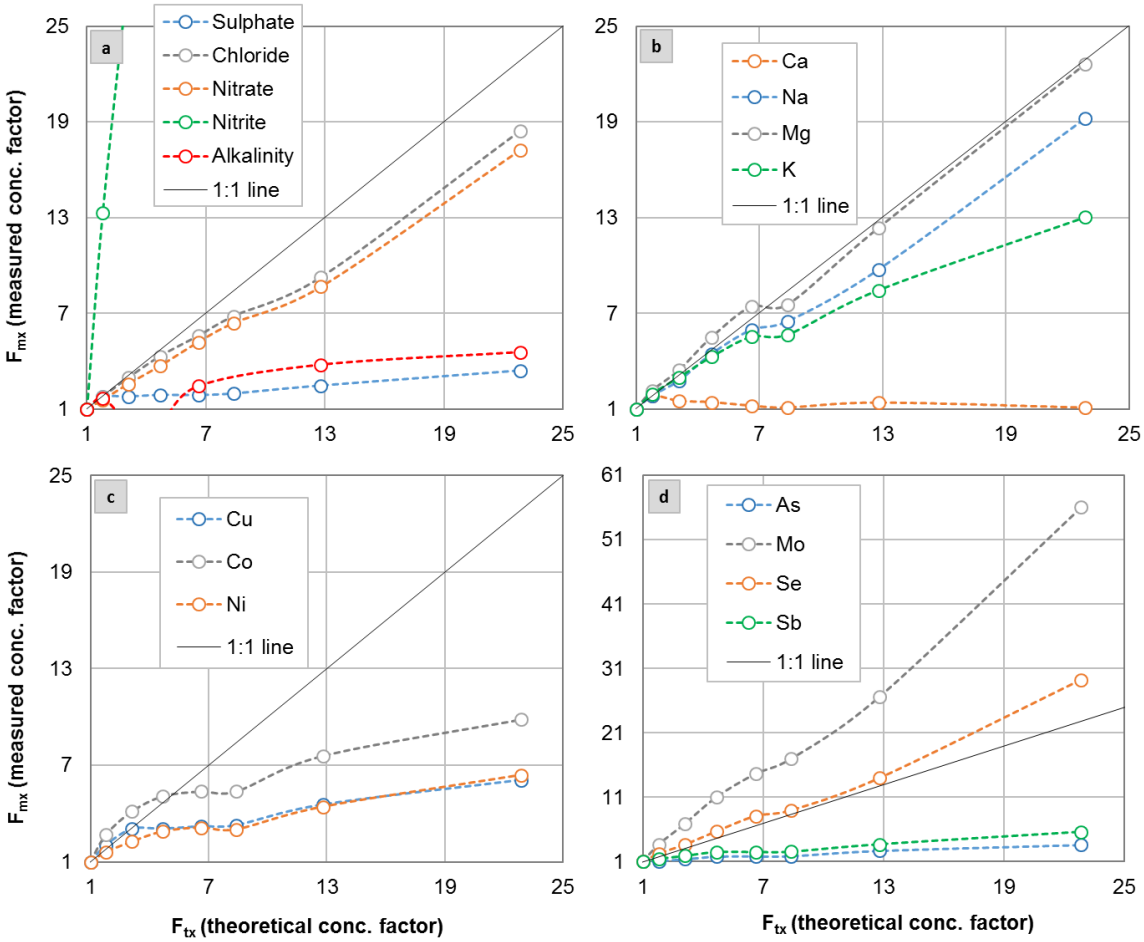

Figure 2 *Theoretical versus measured concentration factors for selected dissolved species in water samples from the bench-scale tailings pond evaporation experiment*

to assess the solid-phase secondary phase data is by comparison with the mass balance budget (i.e., geochemical loads) in the evolving brine and the total mass lost from solution for each species through attenuation mechanisms. The total mass lost from solution due to geochemical processes can be calculated as the sum of geochemical loads lost during all evaporation increments accounting for the dissolved mass lost as a result of sample collection. A geochemical load L is hereby defined as:

$$L = C \times V \qquad \text{(eq. 5)}$$

Theoretically, using this approach the relative impact of secondary mineral precipitation and adsorption on the individual dissolved species can be constrained. Furthermore, comparison of the total mass lost throughout the experiment with the mass budget of the secondary precipitates provides insight into partitioning elemental behaviour into this phase and the impact of its formation on the water chemistry. However, it was observed that the collected secondary precipitate contained impurities of tailings likely causing contamination in the solid-phase analysis. To assess the magnitude of contamination, the aqua regia digestible solid-phase composition of the secondary precipitate (tab. 3) was compared with that of the tailings material. Assuming that the tailings material is homogeneous and that certain elements will have a negligible concentration in the experimental pond water (and therefore in the pure secondary precipitate phase), the lowest ratio of a precipitate constituent relative to its content in the tailings phase should give an approximation of the degree of tailings contamination in the precipitate phase. Applying this approach to the entire suite of measured elements yielded that tailings impurities make up around 20% of the secondary precipitate mass. A corrected solid-phase composition can hence be calculated as:

$$S_{PC} = S_{P0} - 0.2 \times S_T \qquad \text{(eq. 6)}$$

where S_{PC} and S_{P0} are the corrected and measured solid-phase content for a given species, while S_T is the solid-phase content for the same species in the tailings.

Due to analytical constraints, the precise solid-phase contents of Ca and S in the secondary precipitate are reported as overlimit results (tab. 3), which in consideration of the other analyzed constituents suggests that the predominant secondary mineral phase is gypsum. For the remaining species, the corrected precipitate composition was converted into absolute mass loads (by normalization to an adjusted precipitate mass of 14.4 g) and contrasted with the calculated mass lost from solution during the experiment if the dissolved concentration was consistently above the detection limit (tab. 3). Absolute mass loads of Al, Co, and Ni were found to be greater than those that are apparently attenuated during the evaporation experiment. Notwithstanding analytical limitations and uncertainties related to the total mass of the precipitate, this indicates that the tailings material may selectively act as a source for dissolved constituents as the brine evolves. For Al in particular, the mass contained in the collected precipitated phase by far exceeds the dissolved Al budget in the experimental pond. Since this species is strongly solubility-controlled under neutral conditions and is expected to form a discrete phase rather than partition into gypsum, it is inferred that ionic exchange between the tailings and the pond-water may occur for selected constituents to attain geochemical equilibrium. As such, the low apparent mass load removed from solution for some species should not be considered absolute values but rather represents an overall net budget with a geochemical exchange between the different media constantly occurring (Eugster 1980), depending on the changing geochemical regime. The net addition of Mo loads from the tailings material to the evolving brine supports this finding.

The mass of many other species detected in the precipitate only constitutes a small fraction of the attenuation budget (tab. 3). Notably, the major ions Mg, K, and Na account for less than 10% their respective loads lost during the evaporation experiment indicating that (i) these species are being attenuated by different a means such as physically separated discrete phases and/or adsorption and (ii) the gypsum phase is relatively pure with little fractionation of major cations, other than Ca, occurring.

Table 3 *Composition of solid-phase materials and mass balance of evaporation experiment*

	Tailings	Secondary Precipitate			Total Load removed	Precipitate impact
		Measured	Corrected	Absolute mass		
	ppm/%	*ppm/%*	*ppm/%*	*mg*	*mg*	
Al*	1.8	0.42	0.06	8.84	0.10	8749%
As	5.3	3	1.93	0.03	0.060	46%
Ba	145	31	1.62	0.02	0.56	4%
Ca*	3.9	>15	*N/A*	*N/A*	16649	*AL*
Cd	0.034	0.04	0.03	0.00048	0.00060	80%
Co	27	7.7	2.27	0.033	0.026	124%
Cu	475	104	7.90	0.11	0.16	72%
Fe*	3.4	0.73	0.04	5.75	0.049	*AL*
K*	0.16	0.08	0.05	6.80	488	1%
Mg*	1.7	0.55	0.20	28.87	331	9%
Mn	290	97	38.35	0.55	1.7	32%
Mo	35	10.7	3.53	0.05	-1.2	-4%
Na*	0.050	0.11	0.10	14.38	589	2%
Ni	81	23.8	7.42	0.11	0.093	115%
S*	0.23	>5	*N/A*	*N/A*	44472	*AL*
Sb	0.17	0.11	0.08	0.0011	0.086	1%
Se	<1	<1	*N/A*	*N/A*	0.0013	*AL*
Sr	74	662	647	9.32	88	11%
Zn	23	9	4.42	0.06	0.026	*AL*

Notes: *species reported in % unless otherwise stated; AL = not reported due to analytical limitations; Precipitate impact is calculated as the absolute mass over the load removed per species.

Conclusions

A bench-scale experiment was conducted simulating the evaporating environment of a tailings pond in an arid climate. The key geochemical findings from this experiment are:

- The pH remains circum-neutral and increases slightly from 7.7 to 8.2 over the course of the experiment;
- As to be expected for neutral waters, dissolved Fe and Al concentrations remain low, likely as a result of Fe- and Al-hydroxide precipitation;
- Ca and alkalinity are limited by calcite precipitation early on, where Ca and SO_4 precipitate as visible gypsum shortly after. Other major cations (K, Na, Mg) behave relatively conservatively at the concentrations attained in the experiment but would likely precipitate as distinct phases if the concentration of these species was greater in the initial solution;
- The geochemical behaviour of dissolved trace metals and metalloids is variable in the tailings contact water as evaporation proceeds:
    - Base metals Cu, Co, and Zn are effectively scavenged through co-precipitation with and/or adsorption on secondary phases, most likely Fe-hydroxides;
    - Nitrate is transformed into nitrite and likely removed from solution via denitrification;
    - Metalloids that form oxy-anionic complexes may be attenuated (As, Sb), or behave conservatively (Mo, Se) becoming progressively enriched in the evolving brine. For Mo in particular, a geochemical load may even be added from the solid tailings material. This is interpreted to be a result of desorption or other mobilizing processes related to the slight increase in pH;
- Comparison of the apparent mass loadings removed from solution with the elemental budget in the secondary precipitate indicated that, especially for strongly solubility-controlled species, the ion exchange between tailings and water is required to attain the observed equilibrium concentrations in the final evaporative solution and to account for the calculated mass balance. This shows that the evolving brine chemistry is not solely driven by “one-way” attenuation mechanisms, but adapts to the changing geochemical conditions.

References

Balistrieri, L. S., & Chao, T. T. (1990). Adsorption of selenium by amorphous iron oxyhydroxide and manganese dioxide. Geochimica et Cosmochimica Acta, 54(3), 739-751.

Benison, K. C., & Bowen, B. B. (2013). Extreme sulfur-cycling in acid brine lake environments of Western Australia. Chemical Geology, 351, 154–167.

Bowen, B. B., & Benison, K. C. (2009). Geochemical characteristics of naturally acid and alkaline saline lakes in southern Western Australia. Applied Geochemistry, 24(2), 268–284.

Chapman, B. M., Jones, D. R., & Jung, R. (1983). Processes controlling metal ion attenuation in acid mine drainage streams. Geochimica et Cosmochimica Acta, 47(11), 1957-1973.

Cravotta, C. A. III, & Trahan, M. K. (1999). Limestone drains to increase pH and remove dissolved metals from acidic mine drainage. Applied Geochemistry, 14(5), 581-606.

Deocampo, D. M., & Jones, B. F. (2013). Geochemistry of Saline Lakes. Treatise on Geochemistry: Second Edition (Vol. 7). Elsevier Ltd.

Eugster, H. P. (1980). Geochemistry of evaporitic lacustrine deposits. Annual Review of Earth and Planetary Sciences, 8, 35.

Hutchinson G.E. (1957). A Treatise on Limnology, vol. 1, 1015 pp. New York: Wiley.

Long, D. T., Fegan, N. E., Lyons, W. B., Hines, M. E., Macumber, P. G., & Giblin, A. M. (1992). Geochemistry of acid brines: Lake Tyrrell, Victoria, Australia. Chemical Geology, 96(1-2), 33–52.